Improved Syntheses and Structure of $[Mn^{III}Mn^{IV}(O)_2(phen)_4](ClO_4)_3 \cdot 2CH_3COOH \cdot 2H_2O$

Rajesh Manchanda,† Gary W. Brudvig,* Susan de Gala, and Robert H. Crabtree

Department of Chemistry, Yale University, 225 Prospect Street, New Haven, Connecticut 06511

Received March 16, 1994

Structural and functional modeling of the oxygen-evolving center (OEC) in photosystem II (PS II) has received much attention in recent years.[1−4] The OEC, believed to be a tetranuclear oxomanganese complex, catalyzes the light-induced oxidation of water to dioxygen.[5,6] Studies on high-valent dinuclear oxomanganese clusters, especially the di-μ-oxo bridged Mn^{III}_2, $Mn^{III}Mn^{IV}$, and Mn^{IV}_2 clusters, are particularly relevant, as the OEC has been proposed to be a dimer of di-μ-oxo manganese dimers[5,7] and the active site of Mn-catalase has been proposed to consist of a high-valent oxomanganese dimer.[8,9] Of all the known dinuclear di-μ-oxo $Mn^{III}Mn^{IV}$ complexes, none have been more extensively studied than $[Mn^{III}Mn^{IV}(O)_2(phen)_4](ClO_4)_3$ (**1**, phen = 1,10-phenanthroline) and $[Mn^{III}Mn^{IV}(O)_2(bpy)_4](ClO_4)_3$ (**2**, bpy = 2,2′-bipyridyl).[10−16] While there is a crystal structure for **2**,[10] the structure of **1** has not been determined. Instead, a very similar dimer, $[Mn^{III}Mn^{IV}(O)_2(phen)_4](PF_6)_3 \cdot CH_3CN$ (**3**), has been structurally characterized;[17] however, the two Mn ions were crystallographically equivalent. In this report, we present new syntheses of **1** and the structure of $[Mn^{III}Mn^{IV}(O)_2(phen)_4](ClO_4)_3 \cdot 2CH_3COOH \cdot 2H_2O$ (**1a**). In contrast to the previously published structure of **3**,[17] our structure shows crystallographically distinct Mn^{III} and Mn^{IV} ions which are typical of an electron-localized species. These results are consistent with the observed 16-line EPR signal from **1** and the EXAFS data on **1** (simulated with the structural parameters of **2**).[18]

Our group has been studying the chemistry of high-valent oxomanganese dimers in an effort to better understand their behavior under different conditions.[19,20] The assembly of higher nuclearity oxomanganese clusters from mononuclear or dinuclear complexes has also been observed.[15,21] These reactions provide insight into the possible steps leading to assembly of the tetranuclear manganese complex in the OEC of PS II which has been found to occur in sequential light-driven steps leading to the active OEC.[22,23] In this report, we also present the conditions for generation of the trimeric species $[Mn^{IV}_3O_4(phen)_4(H_2O)_2]^{4+}$ (**4**) by acidification of an aqueous solution solution of **1**.

Experimental Section

Synthetic Methods. $[Mn^{III}Mn^{IV}(O)_2(bpy)_4](ClO_4)_3$ (**1**) and $Mn^{III}(phen)(H_2O)(Cl)_3$ (**6**) were prepared by literature methods[11,24] and gave satisfactory analyses. All the solutions were made in doubly-deionized water. Sulfuric acid (0.1 M) was used as the buffer at pH 2.5 for all measurements unless otherwise stated. The pH was adjusted by using 0.1 M sodium hydroxide.

Improved Synthesis of $[Mn^{III}Mn^{IV}(O)_2(phen)_4](ClO_4)_3$, 1. To a solution of $Mn(OOCCH_3)_2 \cdot 4H_2O$ (1 g, 4 mmol) in 50 mL water was added a solution of phen (1.6 g, 8 mmol) in 30 mL of acetone. The colorless solution turned yellow within 1 min. Glacial acetic acid (2 mL) was added to this yellow solution and the pH of the resulting solution was adjusted to 4.5 by addition of 0.1 M sodium hydroxide. The reaction mixture was stirred for about 30 min. A solution of $KBrO_3$ (3.34 g, 20 mmol) in 30 mL of water was added dropwise to the yellow reaction mixture. There was no immediate color change. After 2 h of stirring, the solution turned dark green. A saturated aqueous solution of $NaClO_4$ (1.6 g, 12 mmol) precipitated a green product. (**Safety Note**: *Perchlorate salts of metal complexes with organic ligands are potentially explosive. Only small amounts of the material should be prepared and these should be handled with great caution!*) This green precipitate was filtered and washed with copious amounts of dry diethyl ether to yield a lustrous green product (yield ~78%). EPR spectroscopy showed the characteristic 16-line spectrum (Figure 1A). IR spectroscopy (KBr pellet) showed the characteristic peaks: 3400 (b), 2185 (m), 1629 (s), 1602 (s), 1580 (s), 1517 (s), 1424 (s), 838 (vs), 716 (s), 653 (m), 638 (m) cm^{-1}.

In an alternate synthesis, $Mn^{III}phen(H_2O)(Cl)_3$ was dissolved in perchloric acid (pH = 2.0) and left undisturbed. Green crystals were formed after the liquids evaporated (yield ~93%). EPR spectroscopy (acetonitrile−toluene) glass showed the characteristic 16-line spectrum (not shown).

Attempted Synthesis of $[Mn^{IV}_3O_4(phen)_4(H_2O)_2]^{4+}$. $[Mn^{III}Mn^{IV}(O)_2(phen)_4](ClO_4)_3$, **1** (from above synthesis) was dissolved in a 1:1 mixture of glacial acetic and nitric acids. The pH of the resulting brown solution was ~2. The solution was filtered and set in small test tubes for slow evaporation. After a few days, a black solid deposited on the walls of the test tubes (yield ~48%). The EPR spectrum of this black solid in acetonitrile−toluene glass showed a 35-line pattern from **4** superimposed on a six-line pattern from Mn^{II} (Figure 1B). The six-line spectrum from Mn^{II} (Figure 1C) was subtracted from the spectrum in Figure 1B to reveal the 35-line hyperfine pattern from **4** (Figure 1D).

Measurements. EPR spectra were recorded on a home-built spectrometer.[25] All X-ray diffraction measurements on the single crystal of **1a** ($C_{52}H_{38}O_{20}N_8Cl_3Mn_2$) were made on a Rigaku AFC5S diffractometer with graphite-monochromated Cu Kα radiation (Table 1).

* To whom correspondence should be addressed.
† Current address: Department of Chemistry, Massachusetts Institute of Technology, 77 Massachusetts Avenue, Cambridge, MA 02139.

(1) Christou, G. *Acc. Chem. Res.* **1989**, *22*, 328.
(2) Pecoraro, V. L. *Photochem. Photobiol.* **1988**, *48*, 249.
(3) Brudvig, G. W.; Crabtree, R. H. *Progress in Inorganic Chemistry* **1989**, *37*, 99.
(4) Wieghardt, K. *Angew. Chem. Int. Ed. Engl.* **1989**, *28*, 1153.
(5) Debus, R. J. *Biochim. Biophys. Acta* **1992**, *1102*, 269.
(6) Brudvig, G. W. *ACS Symposium Ser.* **1994**, in press.
(7) Chan, M. K.; Armstrong, W. H. *J. Am. Chem. Soc.* **1991**, *113*, 5055.
(8) Fronko, R. M.; Penner-Hahn, J. E.; Bender, C. J. *J. Am. Chem. Soc.* **1988**, *110*, 7554.
(9) Khangulov, S.; Sivaraja, M.; Barynin, V. V.; Dismukes, G. C. *Biochemistry* **1993**, *32*, 4912.
(10) Plaskin, P. M.; Stoufer, R. C.; Mathew, M.; Palenik, G. J. *J. Am. Chem. Soc.* **1972**, *94*, 2121.
(11) Cooper, S. R.; Calvin, M. *J. Am. Chem. Soc.* **1977**, *99*, 6623.
(12) Dave, B. C.; Czernuszewicz, R. S.; Bond, M. R.; Carrano, C. J. *Inorg. Chem.* **1993**, *32*, 3593.
(13) Manchanda, R.; Thorp, H. H.; Brudvig, G. W.; Crabtree, R. H. *Inorg. Chem.* **1991**, *30*, 494.
(14) Manchanda, R.; Thorp, H. H.; Brudvig, G. W.; Crabtree, R. H. *Inorg. Chem.* **1992**, *31*, 4040.
(15) Sarneski, J. E.; Thorp, H. H.; Brudvig, G. W.; Crabtree, R. H.; Schulte, G. K. *J. Am. Chem. Soc.* **1990**, *112*, 7255.
(16) Thorp, H. H.; Sarneski, J. E.; Brudvig, G. W.; Crabtree, R. H. *J. Am. Chem. Soc.* **1989**, *111*, 9249.
(17) Stebler, M.; Ludi, A.; Bürgi, H.-B. *Inorg. Chem.* **1986**, *25*, 4743.
(18) Kirby, J. A.; Robertson, A. S.; Smith, J. P.; Thompson, A. C.; Cooper, S. R.; Klein, M. P. *J. Am. Chem. Soc.* **1981**, *103*, 5529.
(19) Manchanda, R.; Brudvig, G. W.; Crabtree, R. H.; Sarneski, J. E.; Didiuk, M. *Inorg. Chim. Acta* **1993**, *212*, 135.
(20) Manchanda, R.; Brudvig, G. W.; Crabtree, R. H. *New J. Chem.* **1994**, *18*, 561.
(21) Philouze, C.; Blondin, G.; Me'nage, S.; Auger, N.; Girerd, J.-J.; Vigner, D.; Lance, M.; Nierlich, M. *Angew. Chem. Int. Ed. Engl.* **1992**, *31*, 1629.
(22) Tamura, N.; Cheniae, G. *Biochim. Biophys. Acta* **1987**, *890*, 179.
(23) Miller, A.-F.; Brudvig, G. W. *Biochemistry* **1989**, *28*, 8181.
(24) Goodwin, H. A. and Sylva, R. N. *Aust. J. Chem.* **1965**, *18*, 1743.
(25) Beck, W. F.; Innes, J. B.; Lynch, J. B; Brudvig, G. W. *J. Magn. Reson.* **1991**, *91*, 12.

0020-1669/94/1333-5157$04.50/0

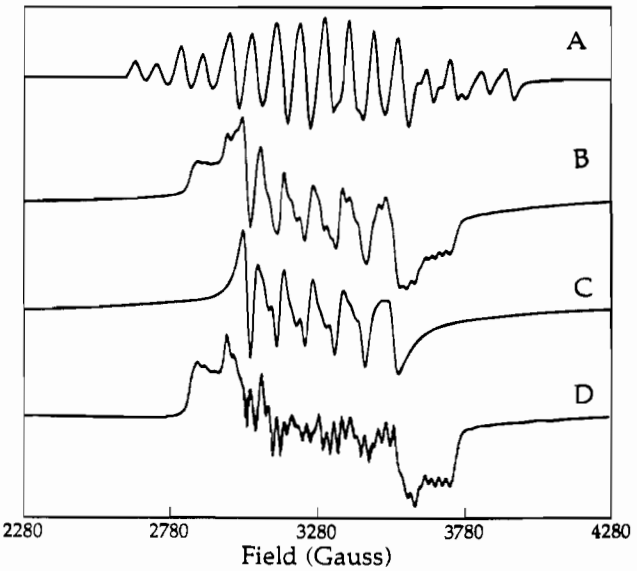

Figure 1. EPR spectrum of (A) **1** in acetonitrile–toluene glass; (B) **4** (in acetonitrile–toluene glass) showing contributions both from the trimeric species and Mn^{II}; (C) $MnCl_2$ in water–ethylene glycol glass; (D) scaled difference of parts B and C revealing the hyperfine structure (~35-line pattern) typical of an antiferromagnetically coupled trimeric oxomanganese cluster.[15] The conditions were as follows: temperature = 10.0 K, microwave frequency = 9.1 GHz, microwave power = 1 μW, field modulation frequency = 100 kHz, field modulation amplitude = 20 G.

Table 1. Crystallographic Data for $[Mn^{III}Mn^{IV}(O)_2(phen)_4](ClO_4)_3 \cdot 2CH_3COOH \cdot 2H_2O$ (**1a**)

chem formula = $C_{52}H_{38}O_{20}N_8Cl_3Mn_2$	fw = 1311.15
a = 14.662(2) Å	space group = $P\bar{1}$ (No. 2)
b = 17.235(3) Å	T = 23 °C
c = 11.956(2) Å	λ = Cu Kα (1.54178 Å)
α = 99.56(1)°	μ = 58.97 cm^{-1}
β = 109.32(1)°	ϱ_{calc} = 1.593 g/cm^3
γ = 99.40(1)°	R^a = 6.5%
V = 2733.0(9) Å^3	$R_w{}^a$ = 7.2%
Z = 2	

$^a R = \Sigma(|F_o| - |F_c|)/\Sigma|F_o|$, $R_w = [(\Sigma w(|F_o| - |F_c|)^2/\Sigma wF_o^2)]^{1/2}$.

Data Collection. Cell constants and an orientation matrix for data collection, obtained from a least-squares refinement using the setting angles of 25 carefully centered reflections in the range 56.90° < 2θ < 71.81°, correspond to a triclinic cell with dimensions a = 14.662(2) Å, b = 17.235(3) Å, c = 11.956(2) Å, α = 99.56(1)°, β = 109.32(1)°, γ = 99.40(1)°, and V = 2733.0 (9) Å^3. For Z = 2 and formula weight (fw) = 1311.15, the calculated density is 1.593 g/cm^3. On the basis of packing considerations, a statistical analysis of intensity distribution, and the successful solution and refinement of the structure, the space group was determined to be $P\bar{1}$ (No. 2).

The data were collected at a temperature of 23 ± 1 °C using the ω–2θ scan technique to a maximum 2θ value of 120.1°. ω scans of several intense reflections made prior to data collection had an average width at half-height of 0.17° with a take-off angle of 6.0°. Scans of (1.52 + 0.30 tan θ)° were made at a speed of 8°/min (in ω). The weak reflections ($I < 10.0\sigma(I)$) were rescanned (maximum of three rescans) and the counts were recorded on each side of the reflection. The ratio of peak counting time to background counting time was 2:1. The diameter of the incident beam collimator was 0.5 mm and the crystal detector distance was 285.0 mm. The $+h$, $\pm k$, $\pm l$ octants were collected.

Data Reduction. Of the 8523 reflections which were collected, 8154 were unique (R_{int} = 0.030). The intensities of three representative reflections, which were measured after every 150 reflections, declined by 52.00%. A linear correction factor was applied to the data to account for this phenomenon. The linear absorption coefficient for Cu Kα is 59.0 cm^{-1}. An empirical absorption correction using the program DIFABS[26] was applied which resulted in transmission factors ranging from 0.83 to 1.43. The data were corrected for Lorentz and polarization effects, but no corrections for extinction were made.

Structure Solution and Refinement. The structure was solved by direct methods[27] (SHELXS). The non-hydrogen atoms were refined anisotropically. The perchlorate ions displayed variations in the Cl–O distances; however, attempts to model these variations in terms of disorder were unsuccessful. The hydrogen atoms were included in calculated positions and not refined. The final cycle of full-matrix least-squares refinement was based on 5432 observed reflections ($I > 3.00\sigma(I)$) and 766 variable parameters and converged (largest parameter shift was 0.00 times its esd) with unweighted agreement factors of $R = \Sigma(|F_o| - |F_c|)/\Sigma|F_o| = 0.065$ and $R_w = [(\Sigma w(|F_o| - |F_c|)^2/\Sigma wF_o^2)]^{1/2} = 0.072$.

The standard deviation of an observation of unit weight was 3.11. The weighting scheme was based on counting statistics and included a factor (p = 0.02) to downweight the intense reflections. Plots of $\Sigma w(|F_o| - |F_c|)^2$ versus $|F_o|$ reflection order in data collection, (sin θ)/λ, and various classes of indices showed no unusual trends. The maximum and minimum peaks on the final difference Fourier map corresponded to 0.76 and −0.62 e/Å^3, respectively.

Neutral atom scattering factors were taken from Cromer and Waber.[28] Anomalous dispersion effects were included in F_{calc}; the values of $\Delta f'$ and $\Delta f''$ were those of Cromer.[28] All calculations were performed using the TEXSAN[29] crystallographic software package of Molecular Structure Corp.

Results and Discussion

In previous syntheses of **1**, $KMnO_4$ has been employed both as an oxidizing agent and a source of Mn.[11] The ratio of Mn^{II} and Mn^{VII} was such that there was no excess of either. The fact that the reduction potential of $KMnO_4$ is highly pH dependent (eq 2) limits the range of the pH available for syntheses; also, at higher pH values, insoluble MnO_2 is formed. The pK_a for ligands like bpy and phen is near 4.5,[24] which allows the use of permanganate but gives low yields, as excess Mn^{II} is generated during the reaction. In an alternate synthesis, bromate ions were employed as an oxidant. The electrochemical potentials for bromate and permanganate are quite similar (eqs 1 and 2):

$$BrO_3^- + 6H^+ + 6e^- \rightarrow Br^- + 3H_2O$$

$$E = 1.44 \text{ V (vs NHE)} \quad (1)$$

$$MnO_4^- + 8H^+ + 5e^- \rightarrow Mn^{2+} + 4H_2O$$

$$E = 1.49 \text{ V (vs NHE)} \quad (2)$$

Bromate is reduced to aqueous bromide ions (eq 1) that can be removed by washing. Additionally, the solubility of bromate in water is as good as that of permanganate. The yield of **1** with this procedure (Scheme 1) was ~78% along with a higher purity than the product obtained by permanganate oxidation (there was no contamination by Mn^{II} as seen by EPR spectroscopy) (Figure 1A). Other synthetic routes to **1** are known.[21] Girerd *et al.* have reported that $Mn^{III}(bpy)(H_2O)Cl_3$ (**5**) yields a novel tetranuclear oxomanganese cluster with perchloric acid.[21] Perchloric acid was considered to act as an oxidant and at the same time provide the perchlorate counterions (although the

(26) Walker, N. and Stuart, D. *Acta Crystallogr.* **1983**, *A39*, 158.
(27) Sheldrick, G. M. In *Crystallographic Computing 3*; Oxford University Press, 1985; pp 175.
(28) Cromer, D. T. and Waber, J. T. in *International Tables for X-ray Crystallography;* The Kynoch Press: Birmingham, England, 1974, Vol. IV.
(29) Molecular Analysis Package, Molecular Structure Corp., The Woodlands, TX, 1989.
(30) Basolo, F.; Dwyer, F. P. *J. Am. Chem. Soc.* **1954**, *76*, 1454.

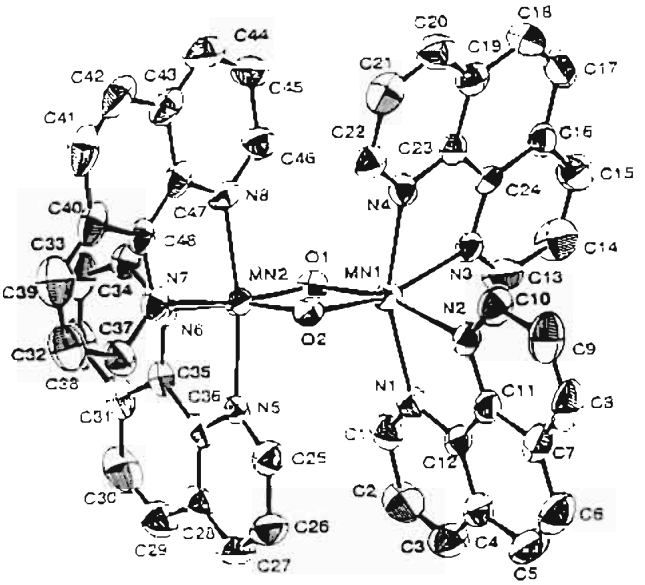

Figure 2. ORTEP diagram of $[Mn^{III}Mn^{IV}(O)_2(phen)_4]^{3+}$ (**1a**).

Scheme 1

$$Mn^{II}(OOCCH_3)_2 + phen + KBrO_3 \xrightarrow[(pH = 4.5)]{\text{Acetate buffer}} [Mn^{III}(phen)(Cl)_3(H_2O)]$$

6

$$\xrightarrow[H^+, O_2]{} [Mn_2^{III,IV}O_2(phen)_4]^{3+}$$

1

Table 2. Selected Bond Distances and Bond Angles in $[Mn^{III}Mn^{IV}(O)_2(phen)_4](ClO_4)_3{\cdot}2CH_3COOH{\cdot}2H_2O$ (**1a**)[a]

selected distances (esd)		selected angles (esd)	
Mn1—Mn2	2.711 (2)	Mn1—O1—Mn2	97.3 (2)
Mn1—O1	1.837(4)	Mn1—O2—Mn1	96.4 (2)
Mn2—O1	1.773(4)	O1—Mn1—O2	81.1 (2)
Mn1—O2	1.859 (4)	O1—Mn2—O2	85.2 (2)
Mn2—O2	1.777 (4)	N1—Mn1—O1	105.7 (2)
Mn1—N1	2.220 (5)	N2—Mn1—O1	164.5 (2)
Mn1—N2	2.123 (6)	N3—Mn1—O1	96.2 (2)
Mn1—N3	2.123 (6)	N4—Mn1—O1	105.7 (2)
Mn1—N4	2.240 (5)	N5—Mn2—O2	89.8 (2)
Mn2—N5	2.036 (5)	N6—Mn2—O2	169.5 (2)
Mn2—N6	2.087 (5)	N7—Mn2—O2	94.4 (2)
Mn2—N7	2.104 (6)	N8—Mn2—O2	96.6 (2)
Mn2—N8	2.034 (5)		
Cl1—O5	1.414 (7)		
Cl3—O11	1.280 (1)		

[a] All distances are measured in angstroms and the angles in degrees.

reaction was done aerobically). In our case, $Mn^{III}(phen)(H_2O)Cl_3$ (**6**), upon acidification (pH = 2) with perchloric acid, yielded **1** almost quantitatively. This route is a straightforward synthetic procedure for the generation of **1** in good yield.

Dark brown prisms of $[Mn^{III}Mn^{IV}(O)_2(phen)_4](ClO_4)_3{\cdot}2CH_3COOH{\cdot}2H_2O$ (**1a**) were obtained from an aqueous acidic solution (containing nitric and acetic acids, pH = 2) of **1**. The molecular structure of **1a** is shown in Figure 2. The site symmetry of the complex is 1, implying that the two Mn ions are crystallographically unique. The inequivalency of the two Mn ions in **1a** arises from the fact that the complex is a mixed-valent oxomanganese dimer with a Jahn–Teller distorted d^4 (Mn^{III}) ion and a normal d^3 (Mn^{IV}) ion. The geometry around Mn1 (Mn^{III}) is typical of an axially elongated d^4 ion (Tables 2 and 3) (e.g. the $Mn-N_{ax}$ distances are 0.12 Å longer than the $Mn-N_{eq}$ distances), while the distances are within the range for a normal d^3 ion for Mn2 (Mn^{IV}) ($Mn-N_{ax}$ are 0.06 Å longer than $Mn-N_{eq}$) (Tables 2 and 3). The intermetal distance in **1a** is 2.711 Å; EXAFS studies on **1**[18] had predicted distances around the Mn ions similar to what we actually observe for **1a**. The two fitting models, e.g. the Teo–Lee and the Hodgson–Donaich models used to fit the EXAFS data on **1**, estimated the Mn—Mn distance to be ~2.699 Å while the Mn—O distance was estimated to be ~1.811 Å; the fit to the Mn—N distances could not be obtained.[18] Additionally, the EXAFS data were modeled based on the known structure of **2**. In fact, the bond distances of **2** and **1a** show marked similarity to each other (Table 3).

Table 3. Comparison of the Distances (Å) around the Mn Ions in $[Mn^{III}Mn^{IV}(O)_2L_4](X)_3$

bonded atoms	**1a**, L = phen, $X = ClO_4$ (296 K)	**2**,[10] L = bpy, $X = ClO_4$	**3**,[17] L = phen, $X = PF_6$ (100 K)
$Mn^{III}—Mn^{IV}$	2.711	2.716	2.700
$Mn^{III}—O1$	1.837	1.853	1.808
$Mn^{III}—O2$	1.859	1.856	1.820
$Mn^{III}—N1ax$	2.220	2.207	2.128
$Mn^{III}—N4ax$	2.240	2.226	2.129
$Mn^{III}—N2eq$	2.123	2.129	2.090
$Mn^{III}—N3eq$	2.123	2.134	2.120
$Mn^{IV}—O1$	1.773	1.784	1.820
$Mn^{IV}—O2$	1.777	1.784	1.808
$Mn^{IV}—N5ax$	2.034	2.028	2.217
$Mn^{IV}—N8ax$	2.036	2.016	2.129
$Mn^{IV}—N6eq$	2.104	2.075	2.090
$Mn^{IV}—N7eq$	2.087	2.075	2.120

In a previous report, Stebler *et al.*[17] have determined the structure of a related complex, $[Mn^{III}Mn^{IV}(O)_2(phen)_4](PF_6)_3{\cdot}CH_3CN$ (**3**), but the two Mn ions (e.g. Mn^{III} and Mn^{IV}) were found to be crystallographically equivalent. The equivalency of the Mn ions could be explained by three different possibilities: (1) the observed structure may result from a superposition of a $Mn^{III}—Mn^{IV}$ and a $Mn^{IV}—Mn^{III}$ (class I, static disorder), (2) the rate of electron transfer between the two metal centers may be faster than the measurement time scale and, thereby, the two Mn ions appear to be equivalent (class II, dynamic disorder), or (3) the two ions may be chemically equivalent, i.e. the d-electrons are totally delocalized over the two metal centers (class III, ordered structure). After a rigorous analysis of the thermal displacement parameters, it was concluded that possibilities 1 and 2 could not be distinguished, while 3 was ruled out.[17]

On the other hand, Robin and Day classify mixed-valent (III,IV) di μ-oxo manganese dimers as class I: the two Mn ions have localized d-electrons and, hence, are structurally distinguishable. For example, **2** shows a different coordination environment around each of the Mn ions (a Jahn–Teller distorted Mn^{III} and a normal Mn^{IV}). Moreover, the EPR spectrum of **1** (and **2**) shows the characteristic 16-line pattern, indicating a d-electron-localized species (Figure 1).[3] Even though Stebler *et al.*[17] collected their data at low temperatures (100 and 200 K), the symmetry imposed on the dimer in the unit cell precluded (due to a superposition of two dimers) distinguishing between the two different Mn ions. In our case, there are no complications arising from the symmetry of the complex in the unit cell, and the coordination geometry around each Mn is characteristic of its d-electron count (the average $Mn^{III}—N$ distance is 0.093 Å longer than the average $Mn^{IV}—N$ distance) (Table 3). Our structural observations are, thus, consistent with those observed[10] for **2**, with the EXAFS data,[18] and with the fact that a 16-line EPR spectrum is observed for **1** (and **2**) as expected for a d-electron-localized species. Our results support the conclusion of Stebler *et al.*[17] that the two

Mn ions in **3**, while crystallographically equivalent, are properly represented as superpositions of nonequivalent Mn^{III} and Mn^{IV} atoms.[31]

The angles around the two Mn ions are typical for a $Mn^{III}Mn^{IV}$ di-μ-oxo moiety (see the supplementary material). We find that the phen rings are almost planar with an approximate 2.6° out-of-plane bend. It is noteworthy that the perchlorate counterions are not regular tetrahedra: the Cl—O distances range between 1.28 and 1.414 Å, while the expected average distance (for a regular tetrahedron) is 1.428 Å. There are two acetic acid and two water molecules that cocrystallize; the two acetic acid molecules are crystallographically well-behaved (C—C = 1.45 Å, C—O = 1.37 Å).

Both of the synthetic procedures require that **1** be stable under rigorous reaction conditions. Chelation by phen may be the reason for such stability and complements the observation of slow kinetics for rearrangement upon acidification of **1** observed previously,[20] which implied that the chelate opening is slower for phen than for bpy. Direct acidification of the bpy complex **2** with nitric acid (pH = 1.5) results in the formation of a trimeric species, $[Mn^{IV}_3O_4(bpy)_4(H_2O)_2]^{4+}$ (**7**),[15] but acidification of **1** with nitric acid does not yield an isolable trimeric species; we further studied the effect of different buffer conditions in order to isolate a stable trimeric species. Acetate has been shown to be an effective labile ligand in oxomanganese chemistry.[1,19] Acetate can ligate to high-valent Mn and, then, can be easily replaced by a stronger ligand such as an oxo group.[19] We employed high concentrations of aqueous acetate at low pH with **1** in order to isolate $[Mn^{IV}_3O_4(phen)_4(H_2O)_2]^{4+}$ (**4**). The black solid thus obtained gave the spectrum in Figure 1B which arises from the superposition of the six-line spectrum of Mn^{II} and a multiline spectrum of a second species. The presence of Mn^{II} indicates that either Mn^{II} is cocrystallizing or there is some solution equilibrium which generates Mn^{II}. Subtracting the contribution from Mn^{II} (Figure 1C) revealed the spectrum in Figure 1D which is similar to that previously observed for **7** and is characteristic of an antiferromagnetically coupled trimeric species.[15] The overall process is presented in Scheme 2. Attempts to obtain a single crystal of **4** suitable for X-ray diffraction are currently underway.

(31) This sentence was suggested by a reviewer.

Scheme 2

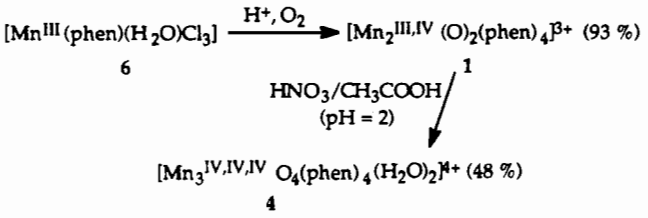

Acknowledgment. This research was funded by the Cooperative State Research Service, U.S. Department of Agriculture, under agreement No. 90-37130-5575 and the National Institutes of Health (Grant GM32715).

Supplementary Material Available: Tables of atomic coordinates and isotropic thermal parameters, U_{ij}s, intramolecular distances and angles, Cartesian coordinates, and torsion or conformation angles and crystal packing diagram of the unit cell (18 pages). Ordering information is given on any current masthead page.